






Comparison of Quantum-Chemical Programs and Methods for the Calculation of Enthalpies of Formation of High-Energy Tetracyclic Compounds

Vadim M. Volokhov¹ , Vladimir V. Parakhin² , Elena S. Amosova¹ ,
David B. Lempert¹ , Vladimir V. Voevodin³ 

© The Authors 2025. This paper is published with open access at SuperFri.org

A comparative study was carried out on the thermochemical properties of a series of high-energy tetracyclic compounds containing amino, cyano, azido, and dinitrophenyl groups. Various quantum-chemical methods were employed to calculate the gas-phase enthalpies of formation, including the B3LYP functional with 6-311+G(2d,p) and cc-pVTZ basis sets, the composite G4MP2 method implemented in Gaussian 09, and a G4MP2-based scheme adapted for implementation in NWChem. The G4MP2 method was used as a reference for accuracy, against which the results of other approaches were evaluated. It is shown that the use of NWChem and reaction-based schemes yields enthalpy values close to those obtained by G4MP2, while significantly reducing computational costs. Structural factors affecting the enthalpy of formation are analyzed, along with differences in the IR absorption spectra. The results confirm the applicability of various theoretical levels for the thermochemical evaluation of promising high-energy materials.

Keywords: high-energy materials, tetracyclic compounds, enthalpy of formation, quantum chemical calculations, isodesmic reactions, atomization, IR spectra, high-performance computing.

Introduction

The enthalpy of formation (ΔH_f°) is one of the key characteristics determining the energy performance of high-energy-density materials (HEDMs) [1–6]. High enthalpy of formation values can be achieved through the incorporation of nitrogen-rich aromatic cores into polycyclic molecular scaffolds [7–10], the energetic properties of which have recently been investigated by our research group [11–18]. Among such structures are tetracyclic compounds – tris(1,2,4-triazolo)-1,3,5-triazines and tris(1,2,3-triazolo)benzenes – the functionalization of which with endothermic nitrogen-containing groups is expected to further increase their enthalpy of formation. To investigate the effect of such combinations, this study focuses on tetracycles bearing amino, cyano, and azido substituents (Fig. 1):

2,6,10-triamino-tris([1,2,4]triazolo)[1,5-a:1',5'-c:1'',5''-e][1,3,5]triazine (**1a**),
2,6,10-tricyano-tris([1,2,4]triazolo)[1,5-a:1',5'-c:1'',5''-e][1,3,5]triazine (**2a**),
2,6,10-triazido-tris([1,2,4]triazolo)[1,5-a:1',5'-c:1'',5''-e][1,3,5]triazine (**3a**),
2,5,8-triamino-tris([1,2,3]triazolo)[1,2-d:3,4-d':5,6-d'']benzene (**1b**),
2,5,8-tricyano-tris([1,2,3]triazolo)[1,2-d:3,4-d':5,6-d'']benzene (**2b**) and
2,5,8-triazido-tris([1,2,3]triazolo)[1,2-d:3,4-d':5,6-d'']benzene (**3b**), which currently remain hypothetical structures,

as well as 2,5,8-tri(2,4-dinitrophenyl)-tris([1,2,3]triazolo)[1,2-d:3,4-d':5,6-d'']benzene (**4**), which has previously been synthesized and characterized as a highly stable and promising, exhibiting exceptionally high thermal stability (with a decomposition onset temperature above 400 °C) and low mechanical sensitivity, with an impact energy threshold of 18 J [19, 20].

¹Federal Research Center of Problems of Chemical Physics and Medicinal Chemistry of the Russian Academy of Sciences, Chernogolovka, Moscow Region, Russian Federation

²N.D. Zelinskiy Institute of Organic Chemistry of the Russian Academy of Sciences, Moscow, Russian Federation

³Research Computing Center of Lomonosov Moscow State University, Moscow, Russian Federation

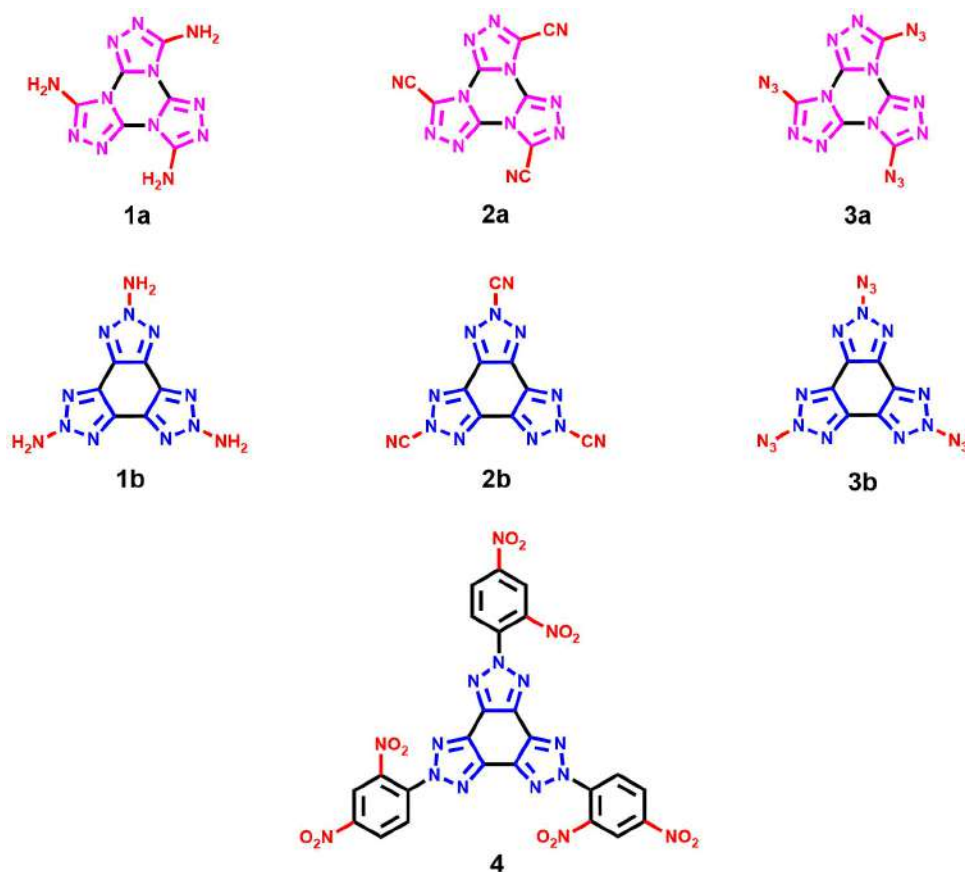


Figure 1. Compounds under investigation – a series of tetracyclic structures **1a,b**, **2a,b**, **3a,b**, and **4**

The article is organized as follows. Section 1 presents the computation methods employed in this work. In Section 2 we discuss the obtained results. Section 3 contains the analysis of method performance on different computational resources. Conclusion summarizes the study and suggests directions for future research.

1. Computation Method

Quantum-chemical calculations were carried out using the GAUSSIAN 09 [21] and NWChem [22] program packages. Geometry optimization was performed using the hybrid density functional B3LYP [23, 24] with the 6-311+G(2d,p) basis set. The stability of the optimized molecular structures was confirmed by calculating vibrational frequencies using analytical first and second derivatives, without applying anharmonic corrections (i.e., the absence of imaginary frequencies). The gas-phase enthalpy of formation of the investigated compounds was calculated using the B3LYP hybrid functional [23, 24] with 6-311+G(2d,p) and cc-pVTZ basis sets [25], as well as the composite G4MP2 [26, 27] method. For the NWChem calculations, a custom module was developed to reproduce the sequence of computational steps of the G4MP2 composite method as described in the literature [26, 28], using the corresponding published equations to obtain the total molecular energy.

$$E_0[G4(MP2)] = CCSD(FC, T)/6 - 31G(d) + \Delta E_{MP2} + \Delta E_{HF} + \Delta E(SO) + E(HLC) + E(ZPE),$$

where CCSD(FC,T)/6-31G(d) is the energy calculation at the triples-augmented coupled cluster level of theory, CCSD(T), with the 6-31G(d) basis set, using frozen core; ΔE_{MP2} and ΔE_{HF} are the energy corrections calculated by the MP2 and HF methods accordingly, $\Delta E(SO)$ is the spin-orbit correction, $E(HLC)$ is the higher-level correction, and $E(ZPE)$ is the zero-point energy.

The IR absorption spectra were calculated using the hybrid density functional B3LYP with the cc-pVTZ basis set. A scaling factor of 0.967 was applied to the computed harmonic frequencies [29].

The enthalpy of formation of the investigated compounds was calculated using two approaches: (I) based on atomization reactions, and (II) based on formation reactions.

The method based on the atomization reaction for the $C_wH_xN_yO_z$ molecule consisted of the following steps:

1. The atomization energy is calculated by subtracting the total energy of the molecule from the sum of the total energies of the atoms, where the total energies are determined by quantum chemical calculations.
2. The enthalpy of formation at 0K is calculated by subtracting the atomization energy from the sum of the enthalpies of formation of gaseous atomic components as stated in the NIST-JANAF database of thermochemical parameters [30].
3. The enthalpy of formation at 298.15K is calculated by introducing thermal corrections both for the molecule and for the atoms, obtained from the quantum-chemical calculation of the molecule or known from experiment (or calculated from experimental molecular constants).

Reaction schemes used for the calculation of enthalpy of formation are shown in Fig. 2. For the benzene-based compounds (**1–3b**, **4**), the total energies of the reactants and products were calculated using the B3LYP hybrid density functional [23, 24] with 6-311+G(2d,p) basis set. For the 1,3,5-triazine-based compounds (**1–3a**), the total energies were calculated using the ω B97XD functional [31] with cc-pVTZ basis set. The atomization enthalpies used in the calculations for all investigated compounds were obtained using the composite G4MP2 method [26, 27].

2. Results and Discussion

2.1. Enthalpy of Formation

Figure 3 presents the main geometric parameters of the optimized structures. Table 1 gathers the results of calculation of the enthalpy of formation by various methods.

The use of the B3LYP functional with the 6-311+G(2d,p) basis set for atomization-based calculations yielded the highest enthalpy of formation values for all compounds under investigation. Based on prior experience, these values appear to be overestimated, as this functional does not provide high accuracy in thermochemical predictions due to its limited treatment of electron correlation, dispersion effects, and basis set incompleteness. Upon replacing the basis set with cc-pVTZ, which had demonstrated good performance in previous studies [17, 18], the resulting values were on average 108 kJ/mol lower compared to those obtained with 6-311+G(2d,p). The root-mean-square deviation (RMSD) of these values from the results obtained using the composite G4MP2 method (excluding compound **4**) was 57 kJ/mol. The smallest deviation – 5 kJ/mol – was observed for compound **2b**. When using the NWChem package with a custom implementation analogous to the G4MP2 method, the RMSD from the G4MP2 results obtained in Gaussian 09 was less than 2 kJ/mol. The module developed for these calculations does not

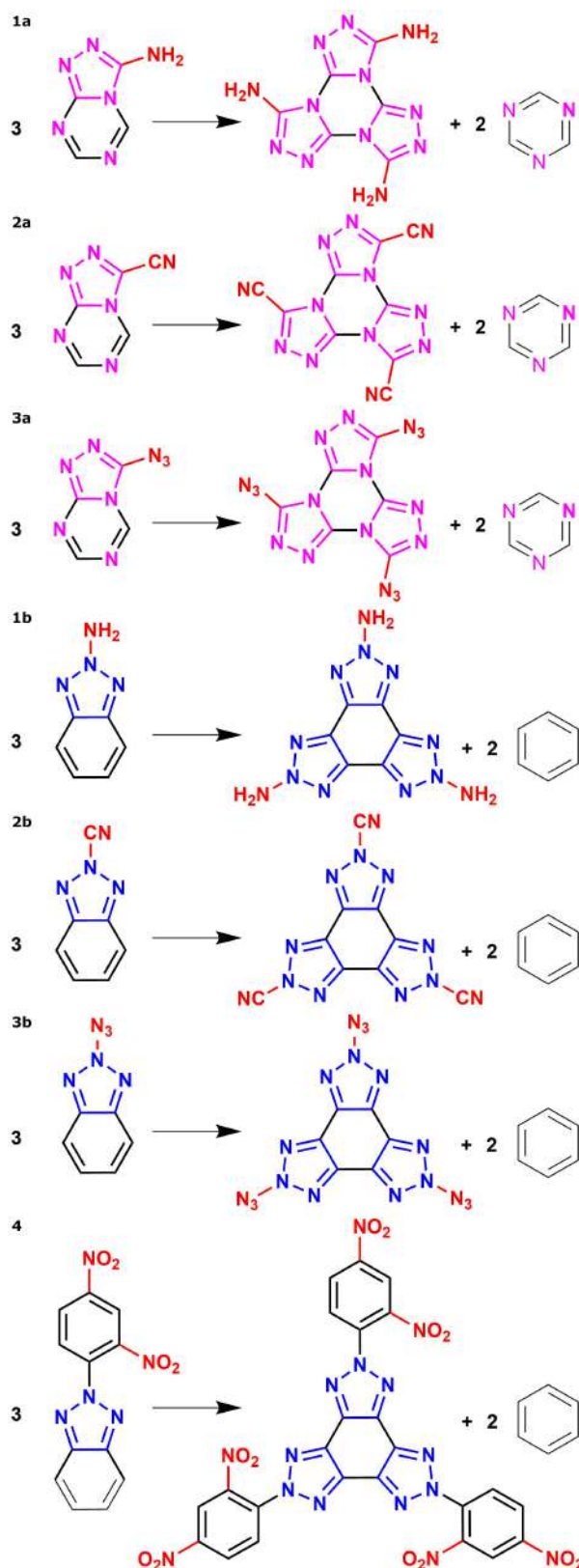


Figure 2. Isodesmic reaction schemes used to calculate the enthalpy of formation of investigated tetracycles **1a,b**, **2a,b**, **3a,b** and **4**

exactly replicate the computational sequence of the G4MP2 method as implemented in GAUSSIAN 09, but rather employs analogous basis sets and functions available in NWChem, which

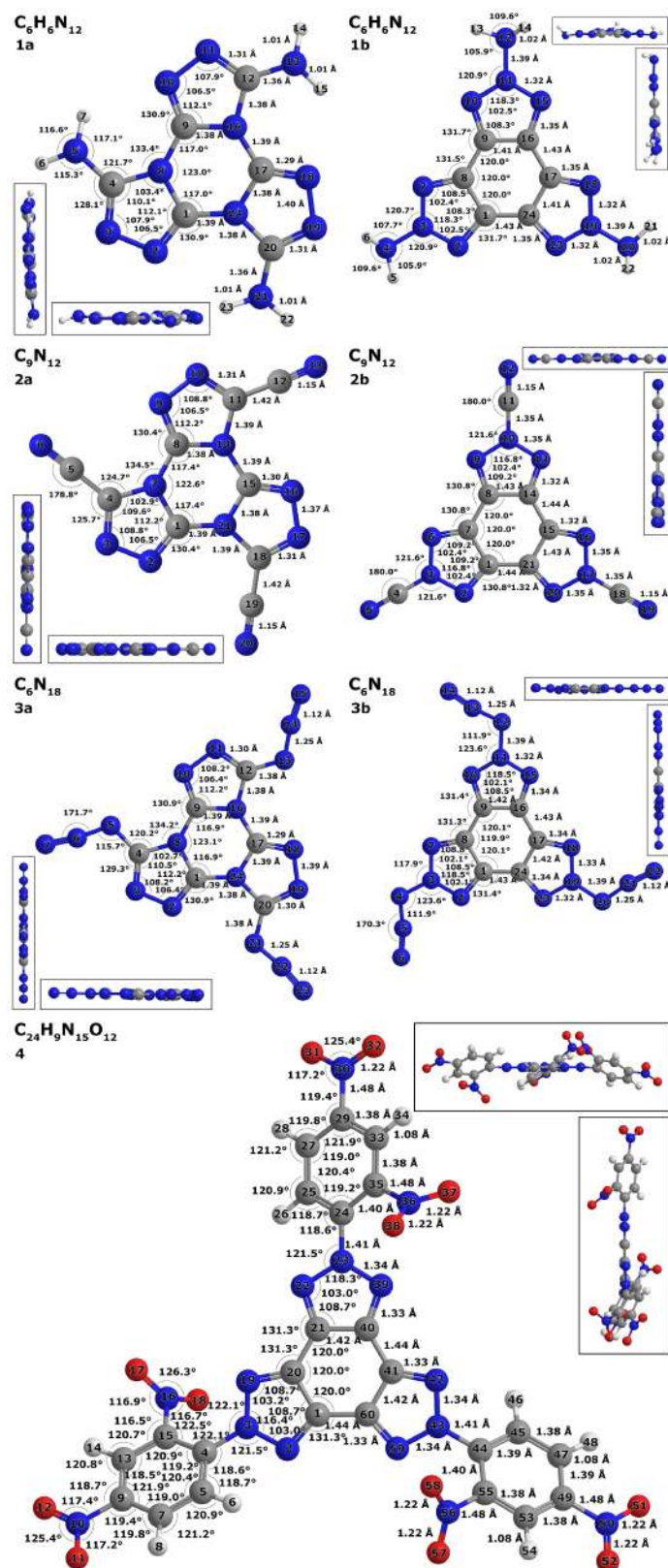


Figure 3. Structures and geometric parameters (in Å and °) of of tetracycles **1a,b**, **2a,b**, **3a,b** and **4** (calculated at B3LYP/6-311+G(2d,p) level)

may also contribute to the observed discrepancies. In the reaction scheme-based calculations, the deviation of the obtained results from the G4MP2 values was less than 2 kJ/mol for most of the

Table 1. Gas-phase enthalpies of formation of tetracycles **1a,b**, **2a,b**, **3a,b**, and **4** calculated by different methods (kJ/mol, (*kJ/kg*))

No	Formula	α	B3LYP	G4MP2	NWChem G4MP2	Reactions	B3LYP/ cc-pVTZ
1a	C ₆ H ₆ N ₁₂	0.00	827.9 (3364.5)	765.6 (3109.6)	764.4 (3104.9)	747.3 (3036.6)	749.5 (3045.7)
2a	C ₉ N ₁₂	0.00	1461.6 (5294.8)	1352.6 (4897.4)	1352.6 (4897.4)	1352.5 (4899.6)	1372.1 (4970.7)
3a	C ₆ N ₁₈	0.00	1874.9 (5785.8)	1849.9 (5706.0)	1850.2 (5707.0)	1842.1 (5684.6)	1754.0 (5412.8)
1b	C ₆ H ₆ N ₁₂	0.00	1169.0 (4750.6)	1116.5 (4535.0)	1117.5 (4539.2)	1118.2 (4543.9)	1096.5 (4455.9)
2b	C ₉ N ₁₂	0.00	1597.7 (5788.1)	1505.2 (5449.9)	1507.5 (5458.3)	1506.0 (5546.0)	1510.0 (5470.5)
3b	C ₆ N ₁₈	0.00	2200.1 (6789.2)	2176.6 (6714.0)	2179.4 (6722.7)	2177.4 (6719.2)	2081.8 (6424.1)
4	C ₂₄ H ₉ N ₁₅ O ₁₂	0.23	1528.3 (2186.3)	– –	– –	1146.1 (1639.5)	1339.0 (1915.5)

Oxygen saturation coefficient: $\alpha = \frac{2O}{4C+H}$

compounds studied. For compounds **1a** and **2a**, the values obtained using reaction schemes were lower than those from G4MP2 by 18 and 8 kJ/mol, respectively. For subsequent comparison and analysis, G4MP2-derived values were used for compounds **1–3a,b**, while for compound **4**, we used the value obtained from the reaction scheme approach.

Previously published literature reports enthalpy of formation calculations for compounds **1a**, **1b**, **2b**, and **3a**, with values very close to those obtained in the present work for the corresponding structures (differences within 1–5 kcal/mol). In particular, Yang [32] reported B3LYP/6-311G(d,p)-level enthalpy of formation values for compounds **1b** and **2b** as 1220.9 and 1602.1 kJ/mol, respectively (literature values have been rounded to one decimal place for consistency with the present results). These values are 52 and 4 kJ/mol higher than those obtained in our work using DFT, and 104 and 97 kJ/mol higher than those obtained using the G4MP2 composite method. The discrepancy between B3LYP-based results may be attributed to our use of a more extended basis set, and possibly to differences in the optimized geometries. The deviation from G4MP2 results falls within the expected error margin of DFT methods for enthalpy of formation calculations. Zeng and co-authors [33] reported a gas-phase enthalpy of formation for compound **3a** of 439.1 kcal/mol (1837.1 kJ/mol), which is approximately 13 kJ/mol lower than the value obtained in this work using the G4MP2 method, and 5 kJ/mol lower than the value calculated using isodesmic reaction schemes. For compound **1a**, the table provided by the authors appears to contain a mix-up in the rows corresponding to the gas-phase enthalpy of formation; the correct value should be 176.5 kcal/mol (738.5 kJ/mol), which is 27 kJ/mol lower than our G4MP2 result and 9 kJ/mol lower than our isodesmic reaction-based value. In their study, the authors also employed reaction schemes, but of a different composition, and the enthalpies of formation for the reactants were calculated using the G3B3 method. Qu and co-authors [34] also reported calculated solid-phase enthalpy of formation values for compounds **1a** and **3a**: 155.3 and 376.1 kcal/mol, respectively (although the article states “kJ/mol”, this appears to be a typographical error). After conversion, these values correspond to 649.8 and

1573.6 kJ/mol, which are 116–276 kJ/mol lower than the gas-phase values obtained in our work. This discrepancy is expected, as the cited literature values correspond to the solid phase and include the contribution of sublimation enthalpy, which the authors estimated using an empirical formula within the framework of the Politzer approach.

The obtained computational results clearly demonstrate the relationship between gas-phase enthalpy of formation and the molecular structure of tris(1,2,4-triazolo)-1,3,5-triazines (**1a**, **2a**, **3a**) and tris(1,2,3-triazolo)benzenes (**1b**, **2b**, **3b**). Most notably, the specific enthalpy of formation of the tetracycles **1a**, **2a**, **3a** and **1b**, **2b**, **3b** follows a consistent increasing trend with respect to the substituent: **1** (–NH₂) < **2** (–CN) < **3** (–N₃). The lowest specific $\Delta H_f^\circ(\text{g})$ values within this series are predicted for the amino derivatives **1a** and **1b** ($\Delta H_f^\circ(\text{g}) \sim 3\text{--}4.5$ MJ/kg), as their structures contain the smallest number of C–N bonds. The enthalpy of formation of the cyano derivatives **2a** and **2b** is significantly higher than that of the corresponding amino compounds due to the presence of three additional C≡N triple bonds. In turn, the azido derivatives **3a** and **3b** exhibit the highest enthalpy of formation values in the series ($\Delta H_f^\circ(\text{g}) \sim 6\text{--}7$ MJ/kg), as their structures incorporate the highly endothermic, energy-rich azido groups –N[–]–N⁺≡N, which are saturated with nitrogen–nitrogen multiple bonds [35].

It is evident that compounds **1a**, **2a**, and **3a**, which contain the 1,2,4-triazole ring, exhibit gas-phase enthalpies of formation (both molar and specific) that are 150–350 kJ/mol (550–1450 kJ/kg) lower than those of their isomeric counterparts **1b**, **2b**, and **3b**, respectively, which incorporate 1,2,3-triazole rings with identical substituents. This difference is primarily attributed to the fact that 1,2,3-triazoles, as previously demonstrated by our group [13], provide the highest gas-phase enthalpy of formation ($\Delta H_f^\circ(\text{g})$) values among triazole isomers due to their greater number of endothermic N–N bonds. In addition, the substituents in compounds **1a**, **2a**, and **3a** are attached to the 1,2,4-triazole rings via carbon atoms, whereas in structures **1b**, **2b**, and **3b**, the functional groups are bonded to the 1,2,3-triazole rings through nitrogen atoms, which further contributes to the increase in $\Delta H_f^\circ(\text{g})$.

Tetracycle **4** exhibits a significantly lower specific $\Delta H_f^\circ(\text{g})$ compared to the compounds discussed above, due to the presence of three dinitrophenyl radicals in its structure, which markedly reduce the enthalpy of formation. This structural feature undoubtedly contributes to the compounds remarkable resistance to external thermal and mechanical impact.

2.2. IR Spectra and Frequency Analysis

The IR absorption spectra of the compounds under investigation are presented in Fig. 4.

Most of the intense bands in the IR spectra of compounds **1a** and **1b** are associated with vibrations in the amino groups. Both spectra exhibit bands corresponding to symmetric and asymmetric N–H *stretching* vibrations. In the 1,3,5-triazine-based compound **1a**, these bands are shifted to higher frequencies – 3565 cm^{–1} and 3439 cm^{–1} – compared to 3470 and 3371 cm^{–1} in the benzene-based isomer **1b**. This shift is likely due to the electronic structure of the triazine ring, which exhibits more pronounced electron-accepting properties than benzene. The N–H *scissoring* vibrations appear around 1575 cm^{–1} in the benzene-based compound and are split into two peaks (1588 cm^{–1} and 1537 cm^{–1}) in the triazine-based isomer. In the region around 1626 cm^{–1} in compound **1a**, the N–H *scissoring* vibrations are coupled with C–N *stretching* modes that connect the amino groups to the triazole fragments. *Wagging* deformations of the amino groups are observed at 1118 cm^{–1} in the benzene-based isomer and at 1087 cm^{–1} in the triazine-based analogue. Compound **1a** also exhibits a characteristic *scissoring* mode at

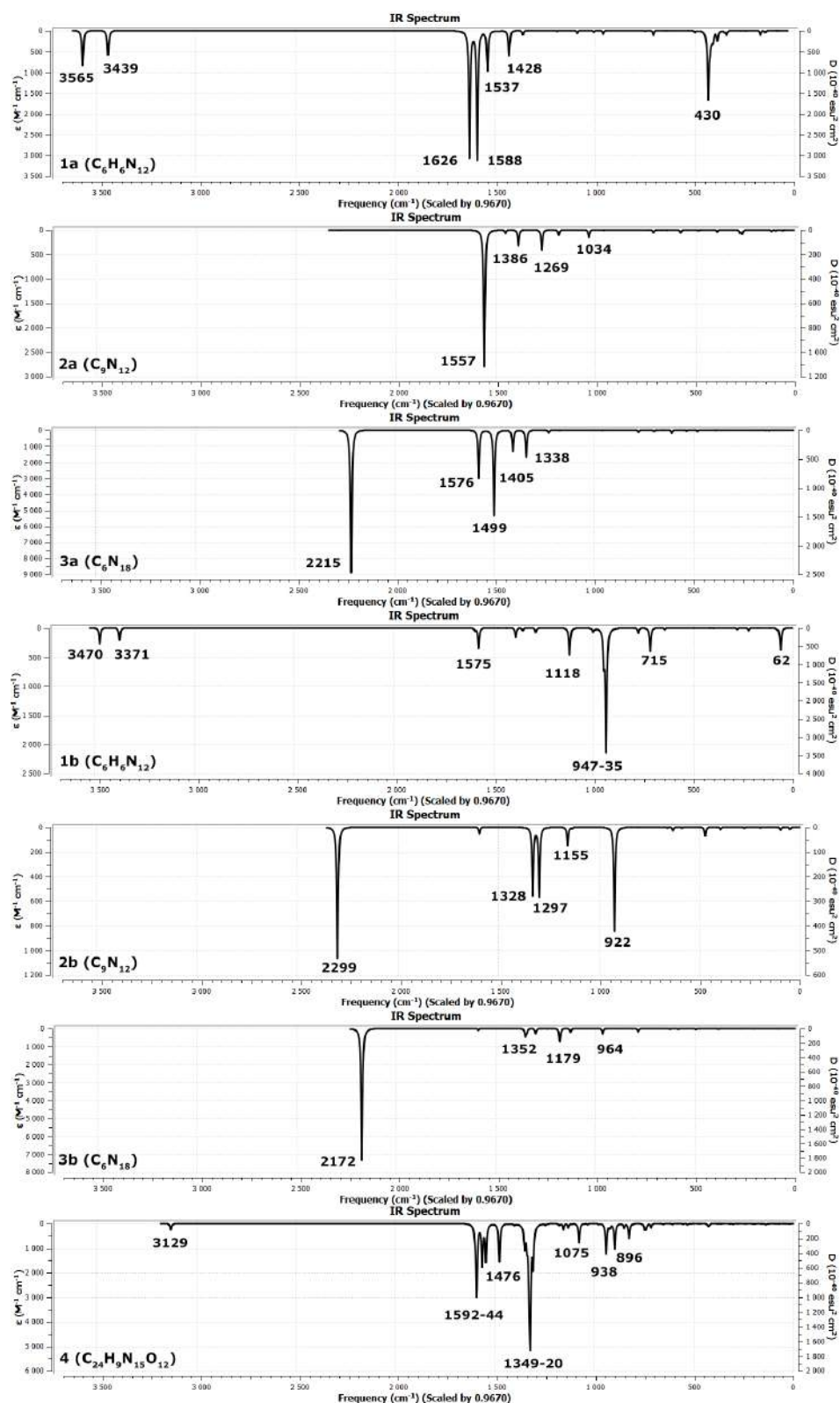


Figure 4. IR absorption spectra of tetracycles **1a,b**, **2a,b**, **3a,b**, and **4** (calculated at the B3LYP/cc-pVTZ level)

1428 cm⁻¹, in which the nitrogen atom of the amino group vibrates in a motion involving both the hydrogen atom and a carbon atom of the triazole ring. In the out-of-plane region, the triazine-based compound exhibits a distinct out-of-plane *wagging* vibration of the NH group at

430 cm^{-1} , whereas the benzene-based isomer displays more diverse out-of-plane *deformations* distributed across the spectrum at 947, 935, and 62 cm^{-1} .

In the IR spectrum of the benzene-based compound **2b**, a distinct band is observed at 2299 cm^{-1} , corresponding to the *stretching* vibrations of the $\text{C}\equiv\text{N}$ bonds in the nitrile groups. In the triazine-based isomer **2a**, similar vibrations are located around 2364 cm^{-1} ; however, their IR intensity is extremely low, resulting in the absence of a visible band in the spectrum. Additional features in the spectrum of compound **2b** include a band at 1297 cm^{-1} , corresponding to $\text{C}-\text{N}$ *stretching* between the triazole and nitrile group, and a peak at 1155 cm^{-1} , which arises from complex *deformation* vibrations involving carbon atoms of the benzene ring and nitrogen atoms of the triazole rings. In the spectrum of the triazine-based isomer **2a**, prominent bands appear at 1269 cm^{-1} , attributed to $\text{C}-\text{N}$ *stretching* within the triazole rings, and at 1034 cm^{-1} , corresponding to $\text{N}-\text{N}$ *stretching* vibrations in the triazole moiety.

Both azido-substituted isomers (**3a** and **3b**) are characterized by *stretching* vibrations of the external $\text{N}-\text{N}$ bonds in the azide groups, observed at 2172 cm^{-1} for the benzene-based compound and at 2215 cm^{-1} for the triazine-based compound. In the spectrum of compound **3b**, a band at 1179 cm^{-1} is also observed, corresponding to the internal $\text{N}-\text{N}$ bond vibrations within the azide group. The spectrum of compound **3a** exhibits the following features: a peak at 1499 cm^{-1} associated with $\text{C}-\text{N}$ *stretching* between the triazole ring and the azide group, and bands at 1405 cm^{-1} and 1338 cm^{-1} , which correspond to combined $\text{C}-\text{N}$ *stretching* vibrations in different fragments (triazine and triazole).

The IR spectrum of compound **4** exhibits several intense absorption bands associated with $\text{C}-\text{H}$ vibrations in the dinitrophenyl rings: 3129–3125 cm^{-1} corresponding to *stretching* vibrations, and 1476 cm^{-1} and 1075 cm^{-1} corresponding to *deformation* modes. The compound also shows characteristic peaks at 1562 cm^{-1} and 1544 cm^{-1} , attributed to asymmetric $\text{N}-\text{O}$ *stretching* vibrations in the nitro groups, and at 823 cm^{-1} , corresponding to *scissoring* deformations in the nitro groups. In addition, prominent intensity peaks are observed in the 1592–1589 cm^{-1} region, associated with $\text{C}-\text{C}$ *stretching* in all benzene rings; at 1349 cm^{-1} , corresponding to $\text{C}-\text{N}$ *stretching* between benzene and the nitro group; at 1337 cm^{-1} and 1326 cm^{-1} , related to $\text{C}-\text{C}$ *stretching* within benzene rings and $\text{C}-\text{N}$ *stretching* in the nitrated fragments; at 1320 cm^{-1} , attributed to combined $\text{C}-\text{N}$ *stretching* vibrations across several parts of the molecule; and at 896 cm^{-1} , corresponding to combined *deformation* vibrations in the peripheral benzene rings.

Most of the benzene-based compounds (**2b**, **3b**, **4**) exhibit characteristic vibrations of the $\text{N}-\text{N}-\text{N}$ fragment within the triazole ring: 922 cm^{-1} for compound **2b**, 964 cm^{-1} for compound **3b**, and 938 cm^{-1} for compound **4**. The spectra of compounds **2b** and **3b** also display similar peaks in the regions of 1328 cm^{-1} and 1352–1344 cm^{-1} , respectively, associated with $\text{C}-\text{C}$ *stretching* vibrations in the benzene rings. The IR spectra of the triazine-based compounds **2a** and **3a** are characterized by strong absorption bands at 1557 and 1576 cm^{-1} , corresponding to $\text{C}-\text{N}$ *stretching* vibrations within the triazine core.

Thus, the IR spectra clearly demonstrate how structural differences – namely, the nature of the substituents and the type of central ring – affect the vibrational behavior of the molecules. All observed bands correspond to vibrations characteristic of the respective functional fragments.

3. Computational Details

Quantum-chemical calculations were carried out using the computing facilities of the Lomonosov Moscow State University Supercomputing Center (project 2312) [36, 37] and the

computational resources of the Federal Research Center of Problems of Chemical Physics and Medicinal Chemistry of the Russian Academy of Sciences. Geometry optimizations for all compounds, as well as calculations using the composite G4MP2 method and its adaptation for the NWChem software package (for all compounds except compound **4**), were performed on the *volta2* partition of the “Lomonosov-2” supercomputer using Intel Xeon Gold 6240 processors (18 cores, 2.60 GHz, 1497.6 GFlop/s) with GPU acceleration (Nvidia Tesla V100, 900-2G500-0010-000, 1246 MHz, 7 TFlop/s).

Geometry optimization using the GAUSSIAN 09 software on the *volta2* partition took approximately 1 hour for compounds **1–3a,b** and 33 hours for compound **4**. G4MP2 calculations for most of the investigated molecules were completed within 11–20 hours; however, the calculation for compound **3a** was not completed due to the 48-hour time limit imposed by the supercomputer. Although the calculation for the structurally similar benzene-based compound **3b** finished successfully in 20 hours, the CCSD(T) step (used to account for electron correlation) proceeded significantly more slowly in case of the triazine derivative, causing the overall computation to exceed the allowed time limit. This may be attributed to the electronic structure of the triazine core combined with azide groups, which could result in poorer convergence or increased complexity in the correlation analysis at the CCSD(T) level. In this case, GAUSSIAN was unable to write a new checkpoint file in time, and upon restart, re-executed the CCSD(T) step from the beginning.

The NWChem software package allows for task distribution across multiple nodes via MPI. For most of the compounds studied in this work, two nodes per task were used, and the calculations took between 2.5 and 6.5 hours. For compound **4**, which has the most complex structure among those considered, eight nodes were employed. However, we encountered technical difficulties during the CCSD(T) step under MPI parallelization, as in our previous studies [18]. These issues may be related to insufficient memory or suboptimal MPI configuration.

DFT calculations using the B3LYP functional with the cc-pVTZ basis set for all compounds were performed using the GAUSSIAN 09 software package on a separate computational resource with the following specifications: Intel(R) Xeon(R) Gold 6140 CPU @2.30 GHz, 259 GB RAM, and 20 TB of disk space. The computations took between 2.5 and 5.5 hours for compounds **1–3a,b**, and 33 hours for compound **4**. The G4MP2 calculation for compound **3a** was also carried out on this system and required approximately 90 hours.

For the enthalpy of formation calculations based on the reaction schemes described above, data obtained from both computational platforms were used. The total calculation time for compounds **1–3a,b** ranged from 3 to 8 hours, and 121 hours for compound **4**. This total runtime is significantly lower than that of G4MP2 calculations on the supercomputer.

Conclusions

The conducted study enabled an assessment of the efficiency of various quantum-chemical approaches for calculating the enthalpy of formation of high-energy tetracyclic compounds. The G4MP2 method was used as a benchmark to evaluate the accuracy of less resource-intensive methods. It was shown that density functional theory (DFT) using the B3LYP functional with the cc-pVTZ basis set significantly reduces the overestimation of thermochemical parameters typical of simpler basis sets and, in some cases, yields enthalpy of formation values close to those obtained with G4MP2. Calculations based on isodesmic reaction schemes demonstrated strong agreement with G4MP2 results while requiring significantly lower computational resources. The

adapted implementation of the G4MP2 scheme in the NWChem software package also showed good agreement with the original implementation in GAUSSIAN 09, while offering greater flexibility for parallel computing on high-performance computing platforms.

At the same time, it should be noted that the G4MP2 calculation for the most complex structure under investigation could not be completed in either GAUSSIAN 09 or NWChem due to runtime limitations and the complexity of the CCSD(T) correlation step. This highlights the limitations of composite methods when applied to large molecules and underscores the relevance of using less computationally demanding approaches such as reaction schemes and DFT methods with carefully selected basis sets.

The analysis of the relationship between molecular structure and thermochemical characteristics confirmed the expected increase in enthalpy of formation along the substituent series $-\text{NH}_2 < -\text{CN} < -\text{N}_3$, as well as the advantage of tetracycles containing 1,2,3-triazole rings over their 1,2,4-triazole-based isomers. IR spectrum calculations showed that the characteristics of the central ring and the nature of functional groups significantly influence the vibrational profile of the compounds.

The obtained results confirm the feasibility of using reaction schemes and adapted high-accuracy methods in the modeling of promising energetic molecules and will serve as a foundation for further evaluation of their energy potential and possible applications.

Acknowledgements

Calculations carried out using the equipment of the shared research facilities of HPC computing resources at Lomonosov Moscow State University [36], were supported by the Russian Science Foundation (project No. 23-71-00005). V.M. Volokhov and E.S. Amosova performed research in accordance with the State Task, state registration No. 124013100856-9. V.V. Parakhin was engaged in the formulation of a scientific problem, literature review, analysis of the results, writing and editing the article. D.B. Lempert performed work in accordance with the State Task, state registration No. 124020100045-5. V.V. Voevodin participated in the quantum-chemical research and the analysis of the results.

This paper is distributed under the terms of the Creative Commons Attribution-Non Commercial 3.0 License which permits non-commercial use, reproduction and distribution of the work without further permission provided the original work is properly cited.

References

1. Rice, B.M., Pai, S.V., Hare, J.: Predicting heats of formation of energetic materials using quantum mechanical calculations. *Combust. Flame* 118, 445–458 (1999). [https://doi.org/10.1016/S0010-2180\(99\)00008-5](https://doi.org/10.1016/S0010-2180(99)00008-5)
2. Byrd, E.F., Rice, B.M.: Improved prediction of heats of formation of energetic materials using quantum mechanical calculations. *J. Phys. Chem. A* 110, 1005–1013 (2006). <https://doi.org/10.1021/jp0536192>
3. Muthurajan, H., Sivabalan, R., Talawar, M.B., *et al.*: Prediction of heat of formation and related parameters of high energy materials. *J. Hazard. Mater.* 133, 30–45 (2006). <https://doi.org/10.1016/j.jhazmat.2005.10.009>

4. Zhong, L., Liu, D., Hu, M., *et al.*: First-principles calculations of solid-phase enthalpy of formation of energetic materials. *Commun. Chem.* 8, 1–7 (2025). <https://doi.org/10.1038/s42004-025-01544-9>
5. Larin, A.A., Muravyev, N.V., Pivkina, A.N., *et al.*: Assembly of tetrazolylfuroxan organic salts: Multipurpose green energetic materials with high enthalpies of formation and excellent detonation performance. *Chem. Eur. J.* 25, 4225–4233 (2019). <https://doi.org/10.1002/chem.201806378>
6. Luk'yanov, O.A., Parakhin, V.V., Shlykova, N.I., *et al.*: Energetic N-azidomethyl derivatives of polynitro hexaazaisowurtzitanes series: CL-20 analogues having the highest enthalpy. *New J. Chem.* 44, 8357–8365 (2020). <https://doi.org/10.1039/D0NJ01453b>
7. Gao, H., Zhang, Q., Sreeve, J.M.: Fused heterocycle-based energetic materials (2012–2019). *J. Mater. Chem. A* 8, 4193–4216 (2020). <https://doi.org/10.1039/c9ta12704f>
8. Wen, L., Wang, Y., Liu, Y.: Data-Driven Combinatorial Design of Highly Energetic Materials. *Acc. Mater. Res.* 6, 64–76 (2025). <https://doi.org/10.1021/accountsmr.4c00230>
9. Kuznetsova, A.N., Leonov, N.E., Anikin, O.V., *et al.*: Parent 1,4-dihydro-[1,2,3]triazolo[4,5-d][1,2,3]triazole and its derivatives as precursors for the design of promising high energy density materials. *New J. Chem.* 49, 311–320 (2025). <https://doi.org/10.1039/D4NJ04427D>
10. Feng, S., Li, Y., Lai, Q., *et al.*: A strategy for stabilizing of N₈ type energetic materials by introducing 4-nitro-1,2,3-triazole scaffolds. *Chem. Eng. J.* 430, 133181 (2022). <https://doi.org/10.1016/j.cej.2021.133181>
11. Volokhov, V.M., Amosova, E.S., Volokhov, A.V., *et al.*: Quantum-chemical calculations of physicochemical properties of high enthalpy 1,2,3,4- and 1,2,4,5-tetrazines annelated with polynitroderivatives of pyrrole and pyrazole. Comparison of different calculation methods. *Comput. Theor. Chem.* 1209, 113608 (2022). <https://doi.org/10.1016/j.comptc.2022.113608>
12. Volokhov, V. M., Parakhin, V. V., Amosova, E. S., *et al.*: Quantum-Chemical Study of Gas-Phase 5/6/5 Tricyclic Tetrazine Derivatives. *Supercomputing Frontiers and Innovations* 10(3), 61–72 (2023). <https://doi.org/10.14529/jsfi230306>
13. Volokhov, V.M., Parakhin, V.V., Amosova, E.S., *et al.*: Quantum-chemical calculations of the enthalpy of formation of 5/6/5 tricyclic tetrazine derivatives annelated with nitrotriazoles. *Russ. J. Phys. Chem. B*, 18(1), 28–36 (2024). <https://doi.org/10.1134/S1990793124010196>
14. Volokhov, V.M., Amosova, E.S., Parakhin, V.V., *et al.*: Quantum-Chemical Study of Some Tris(pyrrolo)benzenes and Tris(pyrrolo)-1,3,5-triazines. In: Voevodin, V., Sobolev, S., Yakobovskiy, M., Shagaliev, R. (eds) *Supercomputing. RuSCDays 2023. Lecture Notes in Computer Science*, vol. 14388, pp. 177–189. Springer, Cham. (2023) https://doi.org/10.1007/978-3-031-49432-1_14
15. Volokhov, V., Amosova, E., Parakhin, V., *et al.*: Quantum-Chemical Simulation of Some Triimidazolobenzenes and Triimidazolo-1,3,5-Triazines. In: Sokolinsky, L., Zymbler, M., Vo-

- evodin, V., Dongarra, J. (eds) Parallel Computational Technologies. PCT 2024. Communications in Computer and Information Science, vol. 2241, pp. 292–303. Springer, Cham (2024). https://doi.org/10.1007/978-3-031-73372-7_21
16. Volokhov, V.M., Parakhin, V.V., Amosova, E.S., *et al.*: Quantum-Chemical Study of Some Trispyrazolobenzenes and Trispyrazolo-1,3,5-triazines. Supercomput. Front. Innov. 11(3), 64–73 (2024). <https://doi.org/10.14529/jsfi240304>
17. Volokhov, V., Amosova, E., Parakhin, V., *et al.*: Quantum-chemical study of unsubstituted tris(triazolo)benzenes and 1,3,5-triazines. In: Parallel Computational Technologies. PCT 2025. Communications in Computer and Information Science (in print).
18. Volokhov, V.M., Parakhin, V.V., Amosova, E.S., *et al.*: Quantum-Chemical Study of High Energy Derivatives of Tris(triazolo)benzenes. Lobachevskii J. Math. 46(8), 3883–3894 (2025). <https://doi.org/10.1134/S1995080225610100>
19. Samsonov, V.A., Volodarskii, L.B., Korolev, V.L., Khisamutdinov, G.K.: Synthesis of benzotriazole. 4-nitrobenzo[1,2-d:3,4-d']bistriazole and 4,4'-dicarboxy-5,5'-1H-1,2,3-triazole. Chem. Heterocycl. Compd. 29, 1169–1171 (1993). <https://doi.org/10.1007/BF00538063>
20. Thottempudi, V., Forohor, F., Parrish, D.A., Shreeve, J.M.: Tris(triazolo)benzene and its derivatives: high-density energetic materials. Angew. Chem. Int. Ed. 51(39), 9881–9885 (2012). <https://doi.org/10.1002/anie.201205134>
21. Frisch, M.J., Trucks, G.W., Schlegel, H.B., *et al.*: Gaussian 09, Revision B.01. Gaussian, Inc., Wallingford CT (2010).
22. Valiev, M., Bylaska, E. J., Govind, N., *et al.*: NWChem: a comprehensive and scalable open-source solution for large scale molecular simulations. Comput. Phys. Commun. 181, 1477 (2010). <https://doi.org/10.1016/j.cpc.2010.04.018>
23. Becke, A.D.: Densityfunctional thermochemistry. III. The role of exact exchange. J. Chem. Phys. 98(4), 5648–5652 (1993). <https://doi.org/10.1063/1.464913>
24. Johnson, B.J., Gill, P.M.W., Pople, J.A.: The performance of a family of density functional methods. J. Chem. Phys. 98(4), 5612–5626 (1993). <https://doi.org/10.1063/1.464906>
25. Dunning, Th.H. Jr.: Gaussian basis sets for use in correlated molecular calculations. I. The atoms boron through neon and hydrogen. J. Chem. Phys. 90(2), 1007–1023 (1989). <https://doi.org/10.1063/1.456153>
26. Curtiss, L.A., Redfern, P.C., Raghavachari, K.: Gaussian-4 theory using reduced order perturbation theory. J. Chem. Phys. 127, 124105 (2007). <https://doi.org/10.1063/1.2770701>
27. Curtiss, L.A., Redfern, P.C., Raghavachari, K.: Gn theory. Comput. Mol. Sci. 1, 810–825 (2011). <https://doi.org/10.1002/wcms.59>
28. Curtiss, L.A., Redfern, P.C., Raghavachari, K.: Gaussian-4 theory. J. Chem. Phys. 126, 084108 (2007). <https://doi.org/10.1063/1.2436888>

29. CCCBDB Vibrational Frequency Scaling Factors. <https://cccbdb.nist.gov/vsfx.asp>, accessed: 2025-04-10
30. NIST-JANAF Thermochemical Tables. <https://janaf.nist.gov/>, accessed: 2025-04-10
31. Chai, J.-D., Head-Gordon, M.: Long-range corrected hybrid density functionals with damped atom-atom dispersion corrections. *Phys. Chem. Chem. Phys.* 10, 6615–6620 (2008). <https://doi.org/10.1039/b810189b>
32. Yang, J.: Theoretical studies on the structures, densities, detonation properties and thermal stability of tris(triazolo)benzene and its derivatives. *Polycycl. Aromat. Compd.* 35(5), 387–400 (2015). <https://doi.org/10.1080/10406638.2014.918888>
33. Zeng, Q., Qu, Y., Li, J., Huang, H.: Theoretical studies on the derivatives of tris([1,2,4]triazolo)[4,3-a:4',3'-c:4'',3''-e][1,3,5]triazine as high energetic compounds. *RSC Adv.* 6, 5419 (2016). <https://doi.org/10.1039/c5ra22524h>
34. Qu, Y., Zeng, Q., Wang, J., *et al.*: Synthesis and properties for benzotriazole nitrogen oxides (BTzO) and tris[1,2,4]triazolo[1,3,5]triazine derivatives. *Int. J. Mater. Sci. Appl.* 7(2), 49–57 (2017). <https://doi.org/10.11648/j.ijmsa.20180702.13>
35. Klapötke, T.M., Krumm, B., Martin, F.A., Stierstorfer, J.: New azidotetrazoles: structurally interesting and extremely sensitive. *Chem. Asian J.* 7, 214–224 (2012). <https://doi.org/10.1002/asia.201100632>
36. Voevodin, V.I.V., Antonov, A.S., Nikitenko, D.A., *et al.*: Supercomputer Lomonosov-2: largescale, deep monitoring and fine analytics for the user community. *Supercomput. Front. Innov.* 6(2), 4–11 (2019). <https://doi.org/10.14529/jsfi190201>
37. Nikitenko, D.A., Voevodin, V.I.V., Zhumatiy, S.A.: Deep analysis of job state statistics on Lomonosov-2 supercomputer. *Supercomput. Front. Innov.* 5(2), 4–10 (2019). <https://doi.org/10.14529/jsfi180201>